Inorganic Chemistry

Article

Is the ³MLCT the Only Photoreactive State of Polypyridyl Complexes?

F. Alary,*,† J.-L. Heully,† L. Bijeire,‡ and P. Vicendo‡

Laboratoire de chimie et physique quantiques, IRSAMC, Université Paul Sabatier, 118 Route de Narbonne, 31062 Toulouse Cedex, France, and Laboratoire des Intéractions Moléculaires, Réactivité Chimique et Photochimique UMR 5623 au CNRS, Université Paul Sabatier, 31062 Toulouse Cedex 07, France

By means of Δ-SCF and time-dependent density functional theory (DFT) calculations on [Ru(LL)₃]²⁺ (LL = bpy = 2,2′-bipyridyl or bpz = 2,2′ -bipyrazyl) complexes, we have found that emission of these two complexes could originate from two metal-to-ligand charge-transfer triplet states (³MLCT) that are quasi-degenerate and whose symmetries are D_3 and C_2. These two states are true minima. Calculated absorption and emission energies are in good agreement with experiment; the largest error is 0.14 eV, which is about the expected accuracy of the DFT calculations. For the first time, an optimized geometry for the metal-centered (MC) state is proposed for both of these complexes, and their energies are found to be almost degenerate with their corresponding ³MLCT states. These [Ru^II(LL)(η_1-LL)₂]²⁺ MC states have two vacant coordination sites on the metal, so they may react readily with their environment. If these MC states are able to de-excite by luminescence, the associated transition (ca. 1 eV) is found to be quite different from those of the ³MLCT states (ca. 2 eV).

1. Introduction

Polypyridyl complexes of d⁶ metal ions such as Ru^II (Figure 1) have attracted the interest of chemists in many different fields especially in the area of nucleic acids photochemistry.[1] They are photoactivable compounds, which may react as photosensitizers via two photochemical processes: type I or type II photoreactions. They can be used as DNA chiral or luminescent probes, chemical photonucleases, and DNA photoreagents. Their long-lived excited states (up to 1 ns) lead to frequent occurrences of specific photoreactivity. For instance, their photoreactivity toward the DNA double-helix stems partly from the redox properties of their triplet metal-to-ligand charge transfer (³MLCT)
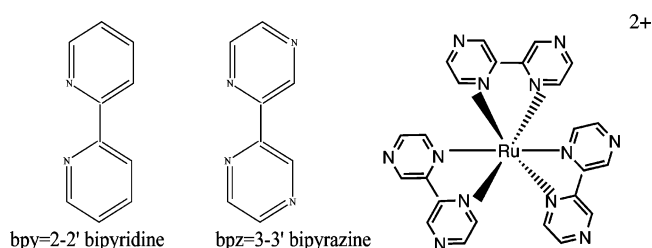

Figure 1. Structure of the ligands considered in this work and sketch of optimized geometry (D_3) of complex [Ru(LL)₃]²⁺ with LL = bpz.

bpy=2-2' bipyridine   bpz=3-3' bipyrazine

excited state.[2] Recently, Bijeire et al.[3a] and Gicquel et al.[3b] have shown that ruthenium complexes with high redox potentials, such as [Ru(TAP)₃]²⁺ and [Ru(bpz)₃]²⁺, may also photosensitize amino acids and protein via electron-transfer processes, leading to novel photochemical reactions such as the formation of a photoadduct with tryptophan or the

* To whom correspondence should be addressed. E-mail: fabienne.alary@irsamc.ups-tlse.fr.
† Laboratoire de chimie et physique quantiques, IRSAMC.
‡ Laboratoire des Intéractions Moléculaires, Réactivité Chimique et Photochimique UMR 5623 au CNRS.
(1) (a) Barton, J. K. *Science* **1986**, *233*, 727−734. (b) Basile, L. A.; Barton, J. K. Metallonucleases: real and artificial. In *Metal Ions in Biological Systems*; Sigel, A., Sigel, H., Eds.; Marcel Dekker: New York, 1989; Vol. 25, pp 31−105. (c) Blasius, R.; Nierengarten, H.; Luhmer, M.; Constant, J. F.; Defrancq, E.; Dumy, P.; van Dorsselaer, A.; Moucheron, C.; Kirsch-DeMesmaeker, A. *Chem.−Eur. J.* **2005**, *11*, 1507−1517.

(2) (a) Jacquet, L.; Davies, R. J. H.; Kirsch-De Mesmaker, A.; Kelly, J. M. *J. Am. Chem. Soc.* **1997**, *119*, 11763−11768. (b) Vicendo, P.; Mouysset, S.; Paillous, N. *Photochem. Photobiol.* **1997**, *65*, 647−655. (c) Sentagne, C.; Chambron, J.-C.; Sauvage, J.-P.; Paillous, N. *J. Photochem. Photobiol. B* **1994**, *26*, 165−174. (d) Lecomte, J. P.; Kirsch-De Mesmaeker, A.; Feeney, M. M.; Kelly, J. M. *Inorg. Chem.* **1995**, *34*, 6481−6491.
(3) (a) Bijeire, L.; Elias, E.; Souchard, J. P.; Moucheron, C.; Kirsch-De Mesmaeker, A.; Vicendo, P. *Biochemistry* **2006**, *45*, 6160−6169. (b) Gicquel, E.; Boisdenghien, A.; Defrancq, E.; Moucheron, C.; Kirsch-De Mesmaeker, A. *J. Chem. Soc., Chem. Commun.* **2004**, *23*, 2764−2765.

modification of the redox state of a metalloenzyme: SOD−Cu/Zn. Because of the very interesting photoreactivity of the ruthenium complexes toward biological targets, we are interested in exploring the nature of the photoreaction occurring between ruthenium complexes with high oxidizing power, such as the $[Ru(bpz)_3]^{2+}$complex, with DNA, and with SOD−Cu/Zn. For this purpose, we have focused our effort on a detailed analysis of the physicochemical characteristics of the ground and low-lying excited states involved in the photoreactivity of two ruthenium complexes, [Ru-(bpy)$_3$]$^{2+}$ and [Ru(bpz)$_3$]$^{2+}$ (bpy = 2,2′-bipyridyl or bpz = 2,2′-bipyrazyl). In the present study, the nature of the triplet excited states has been investigated and we shall provide evidence showing that several states of different character might be involved in the photoreactivity mechanisms. In particular, we show for the first time that both a ^{3}MLCT state with D_3 symmetry and a ^{3}MLCT state with C_2 symmetry exist as true minima, and these states are quasi-degenerated. These results are consistent with the experimental fact that both states are observed. Furthermore, we have performed a time-dependent density functional theory (TD-DFT) study on the triplet D_3 excited state and reproduced the experimental observation that at least four ^{3}MLCT states, lying within 1000 cm^{-1}, plus a metal-centered (MC) state, have to be considered to explain the lower part of the emission spectrum. This MC triplet state, which is perhaps the key of the photochemically induced reactivity of the polypyridyl complexes, has been characterized with small negative eigenvalues on the photoexcited potential energy surface for both of these complexes. For the first time, we have been able to obtain its structure and its relative energy. Surprisingly enough, we found, for both molecules, that they are quasi-degenerate with the ^{3}MLCT states. This provides compelling evidence that many interconversion processes may occur between all of these states. The very unusual geometry (with two monodentate ligands) of these MC states suggests that they could play an important role in the reactivity of these complexes with biological molecules.

This Article is organized as follows: the experimental and computational backgrounds are summarized in sections 2 and 3, respectively. Then elements of the coordination chemistry of bidentate ruthenium complexes are recalled in section 4. Section 5 is devoted to a presentation of the computational methods used in this work. The main body of results and discussion can be found in section 6 (6.1 for the ground state and 6.2 for the excited states, with a subsidiary division into 6.2.1 for results obtained with the Δ-SCF method and 6.2.2 for those obtained in the framework of the TD-DFT approach). Table 7 summarizes all of our results concerning the energies of the different states described in this study.

2. Experimental Background

Light absorption by [Ru(LL)$_3$]$^{2+}$ (LL = bpy or bpz) results in the formation of a Franck−Condon metal-to-ligand charge-transfer (^{1}MLCT) excited state, which undergoes sub-picosecond intersystem crossing to a long-lived ^{3}MLCT excited state. Polypyridyl complexes of the [Ru(LL)$_3$]$^{2+}$ type have been studied intensively, in part because of the debate concerning the description of the lowest

MLCT state. Many observations have been explained by supposing that the excited electron is located on a single ligand, with the two others remaining neutral.[4] In this process, the D_3 symmetry of the ground state is lowered in the triplet states to C_2. Other results obtained from single crystals[5] can be interpreted by a model in which an electron is shared by the three ligands. A recent femtosecond absorption study on [Ru(bpy)$_3$]$^{2+}$ has shown that after 1 ps the MLCT excitation is randomized between the three ligands.[6] For polypyridyl compounds of ruthenium, an additional feature in the photophysical spectrum is the appearance of a low-lying MC triplet state (^{3}MC). For the two complexes [Ru(bpy)$_3$]$^{2+}$ and [Ru-(bpz)$_3$]$^{2+}$, under consideration here, the ^{3}MC states can be populated by thermal activation from ^{3}MLCT states: once formed, they appear to undergo a rapid photodechelation of complexes.

The photophysics of the bipyrazine complex appears to parallel that of its bipyridyl analogue even if some properties are quite different: (i) The ^{3}MLCT transition energies in these complexes are essentially the same; there is a small shift to the blue in the MLCT transition ([Ru(bpy)$_3$]$^{2+}$, 2.13 eV, [Ru(bpz)$_3$]$^{2+}$, 2.16 eV). (ii) Their isoelectronic ligands differ in their σ- and π-bonding characters. Rillema et al.[7] have predicted on the basis of electrochemical reductions that the interaction of the dπ orbital of ruthenium with the π^* orbital of the ligand increases in intensity from bpy to bpz. On the basis of the pK_a value (bipyridine, 5.2; bipyrazine, 0.8), the σ bonding increases from bpz to bpy.

3. Computational Background

Recent applications have shown that the DFT and TD-DFT[8,9] approaches can be powerful and effective computational tools for the study of the photochemistry of these large complexes. Much attention has been devoted to the [Ru-(bpy)$_3$]$^{2+}$ complex. Theoretical DFT[10−12] studies on the electronic structures for the ground state and for the MLCT states of [Ru(bpy)$_3$]$^{2+}$ have already been reported. The [Ru-(bpz)$_3$]$^{2+}$ complex has been less studied because, to our knowledge, only a DFT study of the ground state has been published.[11]

4. Relevant Elements of [Ru(LL)$_3$]$^{2+}$ Coordination Chemistry in Their Different Electronic States

Figure 2 shows a molecular orbital description of these complexes. In their ground state, the distorted octahedral

(4) (a) Dallinger, R. F.; Woodruff, W. H. *J. Am. Chem. Soc.* **1979**, *101*, 4391−4393. (b) Kober, E. M.; Sullivan, B. P.; Meyer, T. J. *Inorg. Chem.* **1984**, *23*, 2098−2104. (c) Saes, M.; Bressler, C.; Abela, R.; Grolimund, D.; Johnson, S. L.; Heimann, P. A.; Chergui, M. *Phys. Rev. Lett.* **2003**, *90*, 047403-1−047403-3. (d) Damrauer, N. H.; Cerullo, G.; Yeh, A.; Boussie, T. R.; Shenk, C. V.; McCusker, J. K. *Science* **1997**, *275*, 54−56.
(5) Felix, F.; Ferguson, J.; Guedel, H. U.; Ludi, A. *J. Am. Chem. Soc.* **1980**, *102*, 4096−4102.
(6) Walli, S.; Davidsson, J.; Modin, J.; Hammarström, L. *J. Phys. Chem. A* **2005**, *109*, 4697−4704.
(7) Rillema, D. P.; Allen, G.; Meyer, T. J.; Conrad, D. *Inorg. Chem.* **1983**, *22*, 1617−1622.
(8) Batista, E. R.; Martin, R. L. *J. Phys. Chem. A* **2005**, *109*, 3128−3133.
(9) Guillemoles, J.-F.; Barone, V.; Joubert, L.; Adamo, C. *J. Phys. Chem. A* **2002**, *106*, 11354−11360.
(10) Daul, C.; Baerends, E. J.; Vernooijs, P. *Inorg. Chem.* **1994**, *33*, 3538−3543.
(11) Zheng, K. C.; Wang, J. P.; Peng, W. L.; Liu, X. W.; Yun, F. C. *THEOCHEM* **2002**, *582*, 1−9.
(12) Xie, Z.-Z.; Fang, W.-H. *THEOCHEM* **2005**, *717*, 179−187.
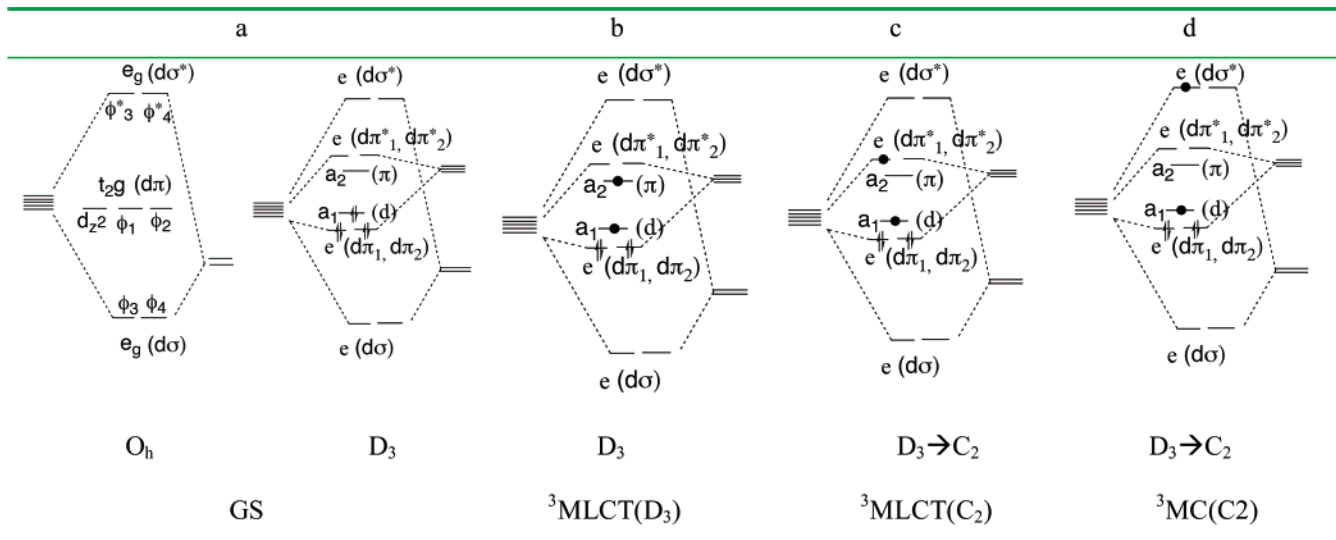(13) Jean, Y. *Molecular orbitals of transition metal complexes*; Oxford University Press: New York, 2005.

Figure 2. (a) Derivation of the d-block orbitals for a RuL$_6$ complex with D_3 symmetry perturbed by π interactions (right-hand side) from those of an octahedral complex when the z axis coincides with a C_3 axis (left-hand side). The d$_{z^2}$, ϕ_1, and ϕ_2 orbitals form the t$_{2g}$ block. The last two (ϕ_1, ϕ_2) are obtained with linear combinations that allow reorientation of the five original d orbitals.[13] In the same way, the two orbitals ϕ_3 and ϕ_4 form the e$_g$ block. (b) Promotion of an electron (●) from the d orbital to the π* orbital giving rise to MLCT excited states of D_3 symmetry. (c) Promotion of an electron from the d orbital to a degenerate dπ* orbital giving rise to MLCT excited states of C_2 symmetry by Jahn−Teller distortion. (d) Promotion of an electron from the metal d orbital to a dσ*orbital giving rise to MC excited states.

bidentate complexes [Ru(LL)$_3$]$^{2+}$ (LL = bpy or bpz) possess a D_3 symmetry. Both of the molecules have a low-spin d^6 metal configuration because the bpy and bpz ligands are known to produce a large ligand field. Figure 2 shows also the electronic configurations of the three important states that are discussed in this work: two ^{3}MLCT states and the ^{3}MC state.

5. Computational Details

In this work, calculations were carried out with the *NWchem*[14] package. The electronic structures of the two complexes were determined via DFT using the B3LYP functional. Calculations are carried out with two different basis sets, namely BS1 and BS2. BS1 consists of a Ru atom described using the relativistic effective core potential (28 core electrons) of Stevens et al.[15] and the associated valence double-ζ basis set; the fourth shell and the 5s electron are described explicitly. No effective core potentials were used for the other atoms: their basis sets are those of Ahlrichs et

al.,[16] which are of double-ζ plus polarization quality. This basis is used for all TD-DFT calculations. In BS2, the Stuttgart relativistic small-core effective potential[17] was used to describe the inner 28 core electrons of Ru, while for the remaining 16 outer shell electrons, a split valence plus polarization basis set whose contraction scheme is (8s7p6d1f)/ [6s5p3d1f] was employed with an exponent of 0.96 for the f function. A triple-ζ plus polarization valence plus polarization basis set was used for C and N atoms and a double-ζ plus polarization basis for H atoms.[17] This basis set of better quality is used for geometrical calculation and vibrational analysis. Use of the *NWchem* package allows us to calculate the electronic excited states and the transition dipole moments via TD-DFT, keeping the lowest 20 singlet and 20 triplet roots for vertical excitations from the ground states. Agreements between our results and experimental data are significantly improved when the asymptotic correction developed by Hirata et al.[18] is used in our calculations. In order to obtain further information on the manifold of the low-lying excited states, we also performed TD-DFT calculations from ^{3}MLCT(D_3) in its optimal geometry. In the Δ-SCF methodology, the triplet states were obtained by the resolution of Kohn−Sham equations under the constraint of a triplet state. This methodology allows us to optimize the geometry of the lowest triplet states but to capture also other triplet states, by starting from appropriate initial guess vectors. For example, we are able to converge to ^{3}MC states by starting with guess vectors obtained from a Hartree−Fock calculation.

(14) Aprà, E.; Windus, T. L.; Straatsma, T. P.; Bylaska, E. J.; de Jong, W.; Hirata, S.; Valiev, M.; Hackler, M.; Pollack, L.; Kowalski, K.; Harrison, R.; Dupuis, M.; Smith, D. M. A.; Nieplocha, J.; Tipparaju, V.; Krishnan, M.; Auer, A. A.; Brown, E.; Cisneros, G.; Fann, G.; Fruchtl, H.; Garza, J.; Hirao, K.; Kendall, R.; Nichols, J.; Tsemekhman, K.; Wolinski, K.; Anchell, J.; Bernholdt, D.; Borowski, P.; Clark, T.; Clerc, D.; Dachsel, H.; Deegan, M.; Dyall, K.; Elwood, D.; Glendening, E.; Gutowski, M.; Hess, A.; Jaffe, J.; Johnson, B.; Ju, J.; Kobayashi, R.; Kutteh, R.; Lin, Z.; Littlefield, R.; Long, X.; Meng, B.; Nakajima, T.; Niu, S.; Rosing, M.; Sandrone, G.; Stave, M.; Taylor, H.; Thomas, G.; van Lenthe, J.; Wong, A.; Zhang, Z. *NWChem, A Computational Chemistry Package for Parallel Computers*, version 4.7; Pacific Northwest National Laboratory: Richland, WA, 2005. Kendall, R. A.; Apra, E.; Bernholdt, D. E.; Bylaska, E. J.; Dupuis, M.; Fann, G. I.; Harrison, R. J.; Ju, J.; Nichols, J. A.; Nieplocha, J.; Straatsma, T. P.; Windus, T. L.; Wong, A. T. High Performance Computational Chemistry: An Overview of NWChem a Distributed Parallel Application. *Comput. Phys. Commun.* **2000**, *128*, 260−283.
(15) Stevens, W. J.; Krauss, M.; Basch, H.; Jasien, P. G. *Can. J. Chem.* **1992**, *70*, 612−630.

(16) Shafer, A.; Horn, H.; Ahlrichs, R. *J. Chem. Phys*. **1992**, *97*, 2571− 2577.
(17) Dolg, M.; Stoll, H.; Preuss, H.; Pitzer, R. M. *J. Phys. Chem*. **1993**, *97*, 5852−5859.
(18) Hirata, S.; Zhan, C.-G.; Aprà, E.; Windus, T. L.; Dixon, D. A. *J. Phys. Chem. A* **2003**, *107*, 10154−10158.

Table 1. Optimized B3LYP Geometries of $[Ru(bpy)_3]^{2+}$ and $[Ru(bpz)_3]^{2+}$ for the Electronic Ground State[a]

bond length/angle	LL = bpy		LL = bpz	
	expt	this work	expt	this work
Ru−N	2.056(2)	2.09(5)	2.05(1)	2.09
>C−N	1.354(4)	1.34	1.33(2)	1.36
>C−C<	1.474(5)	1.47	1.48(4)	1.46
C−N−C	118.0(2)	118.6	118(2)	117.5
N−Ru−N	78.7(1)	77.9	78.6(4)	78.1
N−Ru−N−N	89.1(1)	87.1	90(2)	87.4
N−>C−C<−N	2.2(1)	1.37	4(1)	1.61

[a] The bond distances (in angstroms) and angles (in degrees) are compared to the crystallographic data[20] for the electronic ground state.

The molecular structures and molecular orbital shapes were visualized using *ECCE* software.[19]

6. Results and Discussion

6.1. Ground State. Our results concerning the ground state are reported only for the sake of completeness. The optimized ground-state structures for the two $[Ru(LL)_3]^{2+}$ complexes are presented in Table 1. The experimental geometries are reproduced satisfactorily. The calculated geometry obtained without symmetry constraints shows that the three ligands are indeed equivalent. The largest differences with experiment are observed for the bonds to the central metal atom. These interactions are always overestimated by DFT methods when hybrid functionals are used.[20]

In Figure 3, we report a schematic representation of the energy and character of the frontier orbitals of the two complexes in their ground state. It can be seen that the molecular orbital scheme is nearly the same for the two complexes. The DFT molecular orbitals are quite coherent with the predicted orbital scheme depicted in Figure 2, but when Hartree−Fock orbitals are used, the d orbitals are not the highest ones. The highest-occupied DFT orbitals of symmetry a_1 (d) and e ($d\pi_1$ and $d\pi_2$) are metal-centered. A more pronounced nonbonding character (80% vs 70% of metal character) is shown by the d_{z^2} orbital, named "d" in our work. The lowest unoccupied molecular orbital (LUMO) of a_2 symmetry is purely of ligand character. The two higher LUMOs with e symmetry ($d\pi_1^*$ and $d\pi_2^*$) are predominantly composed of the lowest π^* orbital of two of the three LL fragments, but their metal character is not negligible (ca. 8%). We note that the $d\sigma^*$ orbitals of the two complexes are quite high in the virtual orbital spectrum. The σ-antibonding character between the d orbital of the metal and the lone pair on the N atom is clearly visible in the molecular orbitals $d\sigma^*_1$ and $d\sigma^*_2$ of Figure 3.

Some minor differences between the two complexes in the electronic structure can be noted. The energies of the highest occupied molecular orbital (HOMO) and LUMO are

stabilized in the $[Ru(bpz)_3]^{2+}$ complex, and we also note a small reduction (from 3.64 to 3.52 eV) of the HOMO−LUMO gap on going from bpz to bpy. This trend is consistent with the substitution of CH units by N atoms in the aromatic ring. This trend is also consistent with the change in the donor strength of the ligand: bpy is a stronger donor than bpz, and this increasing field strength causes destabilization of the $d\pi$ molecular orbital. We also want to point out that the difference discussed above is quite consistent with the standard oxidation and reduction potentials of the two complexes. It is more difficult to remove an electron from the HOMO of $[Ru(bpz)_3]^{2+}$, whose E_{ox} is 1.980 V,[21] than from the HOMO of $[Ru(bpy)_3]^{2+}$, whose E_{ox} is 1.270 V.[22] It would be easier to place an electron in the LUMO of $[Ru(bpz)_3]^{2+}$, whose E_{red} is −0.680 V,[22] than in the LUMO of $[Ru(bpy)_3]^{2+}$, whose E_{red} is −1.310 V.[22] A more detailed study of the electrochemical features of these complexes has been undertaken by Stoyanov et al.[22]

6.2. Excited States. 6.2.1. Δ-SCF. In Figure 3, we see two sets of empty molecular orbitals that can be used to describe the excited states. As can be seen in Figure 2b, promotion of an electron from the HOMO to the lowest unoccupied orbital gives rise to a ^{3}MLCT state of D_3 symmetry, i.e., ^{3}MLCT(D_3), whereas the promotion of an electron from the HOMO to one of the degenerate sets of unoccupied orbitals (Figure 2c) could lead to a ^{3}MLCT state of C_2 symmetry, i.e., ^{3}MLCT(C_2). As a consequence, we may observe a change in the symmetry of the complex from D_3 to C_2, as a result of the Jahn−Teller effect. In principle, the Δ-SCF calculation will yield only the lowest triplet states. However, because of the difference in symmetry between the ^{3}MLCT(D_3) and ^{3}MLCT(C_2) states, it is possible to isolate variationnally both of these two states with appropriate initial guess vectors.

6.2.1.1. ^{3}MLCT(D_3). We performed an unrestricted DFT (UKS) calculation to optimize the structure of the triplet state of each complex. Optimizations of the structures were performed without symmetry constraints. Results of the optimization can be found in Table 2. Analysis of the spin density based on Mulliken population analysis (MPA) indicates that in this state the Ru atom keeps one electron while the other electron is delocalized over the three ligands. The values of $\langle S^2 \rangle$ (2.0005) and the spin atomic density confirm that we have obtained a ^{3}MLCT state. Analysis of the vibrational frequencies computed at the same level of theory shows clearly that, for both complexes, they correspond to two true minima on their excited potential energy surface. The two $[Ru(LL)_3]^{2+}$-optimized structures show a D_3 symmetry. The Ru−N bond distance for the two complexes in these ^{3}MLCT states is reduced by 0.01 Å compared to the ground state. We found an energy difference with respect to the ground state (at the triplet geometry) of 2.13 eV for the $[Ru(bpy)_3]^{2+}$ dication and of 2.21 eV for the $[Ru(bpz)_3]^{2+}$ dication: these values agree very well with

(19) Black, G.; Didier, B.; Elsethagen, T.; Feller, D.; Gracio, D.; Hackler, M.; Havre, S.; Jones, D.; Jurrus, E.; Keller, T.; Lansing, C.; Matsumoto, S.; Palmer, B.; Peterson, M.; Schuchardt, K.; Stephan, E.; Sun, L.; Taylor, H.; Thomas, G.; Vorpagel, E.; Windus, T.; Winters, C. *Ecce, A Problem Solving Environment for Computational Chemistry, Software*, version 3.2.5; Pacific Northwest National Laboratory: Richland, WA, 2006.

(20) Rillema, D. P.; Jones, D. S.; Woods, C.; Levy, H. A. *Inorg. Chem.* **1992**, *31*, 2935−2938.

(21) Dürr, H.; Dörr, G.; Zengerle, H.; Curchod, J.-M.; Braun, M. A. *Helv. Chim. Acta* **1983**, *66*, 2652−2655.

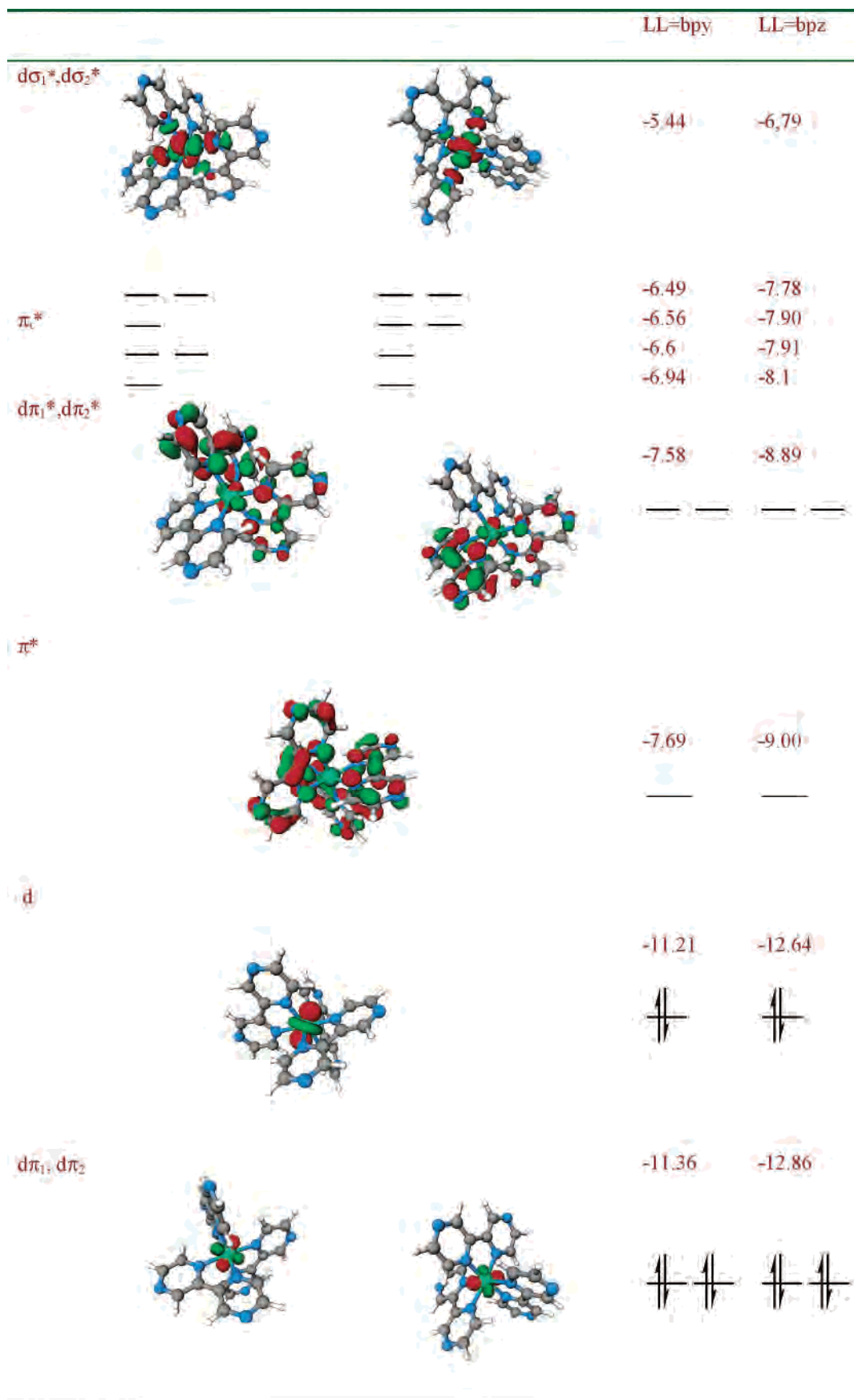(22) Stoyanov, S. R.; Villegas, J. M.; Rillema, D. P. *Inorg. Chem.* **2002**, *41*, 2941−2945.

	LL=bpy	LL=bpz
$d\sigma_1^*, d\sigma_2^*$	-5.44	-6.79
π_c^*	-6.49	-7.78
	-6.56	-7.90
	-6.6	-7.91
	-6.94	-8.1
$d\pi_1^*, d\pi_2^*$	-7.58	-8.89
π_c^*	-7.69	-9.00
d	-11.21	-12.64
$d\pi_1, d\pi_2$	-11.36	-12.86

Figure 3. Isovalue representation of the d-block molecular orbitals of $[Ru(bpz)_3]^{2+}$,[25] and the corresponding eigenvalues (in eV) for $[Ru(bpy)_3]^{2+}$ and $[Ru(bpz)_3]^{2+}$ complexes.

Table 2. Optimized B3LYP Geometries of [Ru(bpy)$_3$]$^{2+}$ and [Ru(bpz)$_3$]$^{2+}$ for the ^{3}MLCT(D_3) and Atomic Spin Density Based on MPA^a

bond length/angle	LL = bpy	LL = bpz
Ru$-$N	2.08	2.08
>C$-$N	1.37	1.37
>C$-$C<	1.45	1.44
C$-$N$-$C	119.4	118.0
N$-$Ru$-$N	78.4	78.3
N$-$Ru$-$N$-$N	85.6	86.0
N$->$C$-$C$<-$N	-2.3	-2.3
atomic spin density	0.33	0.33

^{a} Bond distances (in angstroms) and angles (in degrees).

Table 3. Calculated Bond Length and Angle Values for [Ru(bpy)$_3$]$^{2+}$ and [Ru(bpz)$_3$]$^{2+}$ Complexes in Their ^{3}MLCT(C_2) State and Atomic Spin Density Based on MPA^a

bond length/angle	LL = bpz			LL = bpy		
	c	a	b	c	a	b
Ru$-$N	2.108	2.083	2.078	2.114	2.085	2.077
>C$-$N	1.37	1.37	1.37	1.36	1.37	1.35
>C$-$C<	1.46	1.45	1.45	1.45	1.44	1.44
C$-$N$-$C	119.4	119.4	119.4	118.2	118.0(5)	118.0(5)
N$-$Ru$-$N	77.7	78.7	78.7	77.7	78.6	78.6
N$-$Ru$-$N$-$N	84.	83.6	83.6	84.1	83.7	83.7
N$->$C$-$C$<-$N	5.57	1.20	1.20	6.20	1.62	1.62
atomic spin density	0.40	0.22	0.22	0.42	0.22	0.22

^{a} See Figure 5 for bond ligand descriptions.

the corresponding experimental values, being 2.13^{23} and 2.16 eV,^{24} respectively, though we must note that the emission spectra of polypyridyl complexes are strongly temperature- and solvent-dependent.

The relevant molecular orbitals and their eigenvalues for [Ru(bpy)$_3$]$^{2+}$ and [Ru(bpz)$_3$]$^{2+}$ are shown in Figure 4.

It can be seen from the calculated UKS molecular orbitals that the molecular orbital scheme is nearly the same for the two complexes. As expected, the triplet excited state has d $\rightarrow \pi^*$ character, with the hole located on the d orbital and the electron spread over the three ligands. The MPA also indicates that the electron is shared by the three ligands, respecting D_3 symmetry. This excitation corresponds to the expected HOMO $\rightarrow$ LUMO excitation. After the d $\rightarrow \pi^*$ transition, the Ru atom can be viewed as a metal with an oxidation number of 3 and an electron spread over the ring ligands. The electrostatic interaction between a more positive metallic center and a more negative ligand crown is reinforced, thereby provoking the shortness of the Ru$-$N bond in the ^{3}MLCT(D_3) states. The energies of the frontier molecular orbitals of [Ru(bpz)$_3$]$^{2+}$ are all lower than those of [Ru(bpy)$_3$]$^{2+}$. This suggests, according to Koopman's theorem,^{26} that an electron may be more easily transferred from DNA guanine or protein amino acid to the frontier orbital of the [Ru(bpz)$_3$]$^{2+}$ complex than to the bpy system. For this subject, the elucidation of the photoadduct formation

between a ^{3}MLCT and a DNA base (guanine) or an amino acid (tryptophan) is under investigation.

6.2.1.2. ^{3}MLCT(C_2). Geometry optimization from the ^{3}-MLCT(D_3) state with an initial guess where an electron was put on the dπ_1^* orbital leads to optimized structures that converge toward C_2 symmetry. A schematic representation of the optimized structures of [Ru(bpz)$_3$]$^{2+}$ and [Ru(bpy)$_3$]$^{2+}$ is presented in Figure 6, and the principal geometric parameters are listed in Table 3. For both complexes, the distribution of atomic spin densities on the metallic ions and ligands (see the last line of Table 3) and $\langle S^2 \rangle$ value (2.0059) provide clear evidence that the structures are of the ^{3}MLCT nature. Our results indicate that these ^{3}MLCT(C_2) states are slightly lower in energy than in their D_3 structures for both complexes. The ^{3}MLCT(C_2)$-$^{3}MLCT(D_3) gaps are 10.4 and 7.42 meV for the [Ru(bpy)$_3$]$^{2+}$ and [Ru(bpz)$_3$]$^{2+}$ complexes, respectively. Starting from the MLCT(D_3) triplet structure, a lengthening of the Ru$-$N distance takes place for one of the three ligands (the bond called c in Figure 5). Vibrational analysis revealed that the C_2 structures are also true minima on their respective excited potential energy surface.

If we examine the spin density based on MPA for the two complexes, we find that most of the negative charge resides on the most distant ligand (bond c). This charge distribution is consistent with the C_2 symmetry of these excited states. These results can be related to the localization of an electron on one of the three ligands as observed in some spectroscopic experiments.^{4,6}

The difference in geometry between ^{3}MLCT(D_3) and ^{3}MLCT(C_2) can be rationalized in terms of the shape of the first single occupied molecular orbital (SOMO). In the ^{3}MLCT(C_2) structure, the lowest SOMO orbital, which is clearly of metallic character, has two bonding Ru$-$N contributions ($d = 2.07$ Å), while inspection of the highest SOMO shows that two antibonding interactions can explain the lengthening of two Ru$-$N bonds ($d = 2.11$ Å) compared to the ground state (2.09 Å). Even if experimental evidence of the existence of a ^{3}MLCT(C_2) state is abundant, there is no available experimental structural information for these ^{3}MLCT(C_2) species.

6.2.1.3. ^{3}MC. Accurate experimental information about the energies and the structure of ^{3}MC is very scarce. Van Houten and Watts^{27} have found experimentally that the photoactive ^{3}MC levels lie 3560 cm^{-1} (0.45 eV) above the lowest MLCT state, but Rillema et al.^{28} reported that the ^{3}MC level is lower than the ^{3}MLCT level. In 1982, Durham et al.^{29} suggested that the relative position of the ^{3}MC level cannot be established. In 2001, Thompson et al.^{30} have shown that high-power flash excitation yields both ^{3}MLCT states and a transient ^{3}MC excited state. This photoproduct is

(23) Cook, J. M.; Lewis, A. P.; McAuliffe, G. S. G.; Skarda, V.; Thomson, A. J.; Glasper, J. L.; Robbins, D. J. *J. Chem. Soc., Perkin Trans.* **1984**, *2*, 1293$-$1301.
(24) Haga, M.; Dodsworth, E. S.; Eryavec, G.; Seymour, P.; Lever, A. B. P. *Inorg. Chem.* **1985**, *24*, 1901$-$1906.
(25) For isovalue representation of molecular orbitals of the [Ru(bpy)$_3$]$^{2+}$, see ref 12.
(26) Koopman, T. A. *Physica* **1933**, *1*, 104.

(27) Van Houten, J.; Watts, R. J. *J. Am. Chem. Soc.* **1976**, *98*, 4853$-$4858.
(28) Allen, G. H.; White, R. P.; Rillema, D. P.; Meyer, T. J. *J. Am. Chem. Soc.* **1984**, *106*, 2613$-$2620.
(29) Durham, B.; Caspar, J. V.; Nagle, J. K.; Meyer, T. J. *J. Am. Chem. Soc.* **1982**, *104*, 4803$-$4810.
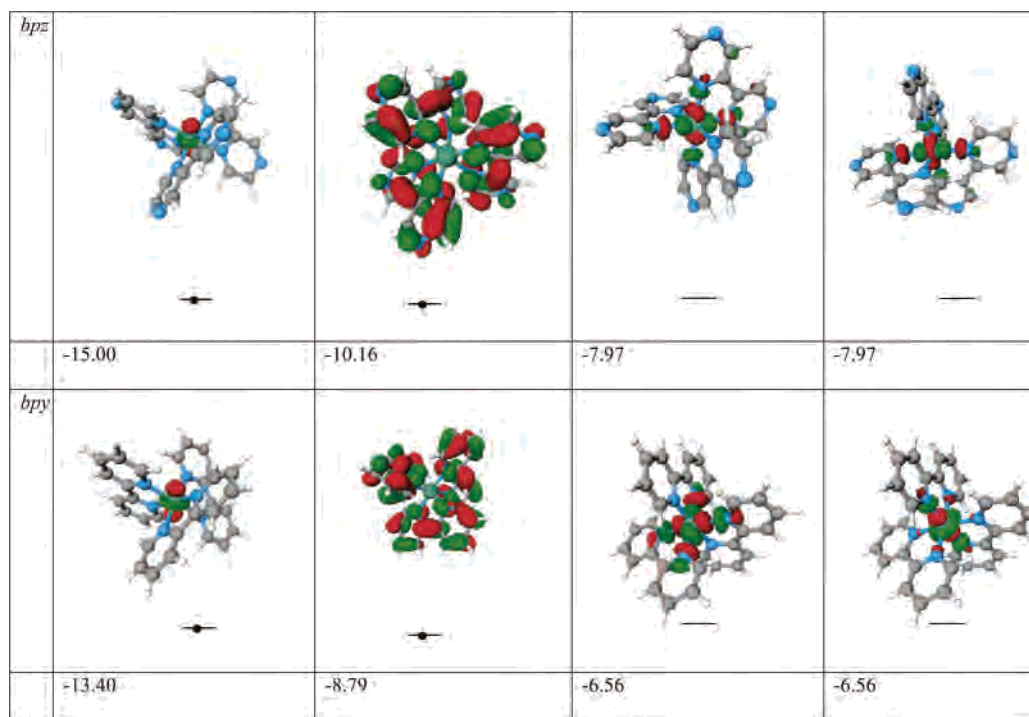(30) Thompson, D. W.; Wishart, J. F.; Brunschwig, B. S.; Sutin, N. *J. Chem. Phys.* **2001**, *105*, 8117$-$8122.

Figure 4. Schematic drawings of the d-block orbitals [Ru(bpy)$_3$]$^{2+}$ and the corresponding eigenvalues of the ^{3}MLCT state of D_3 symmetry for [Ru-(bpy)$_3$]$^{2+}$ and [Ru(bpz)$_3$]$^{2+}$.
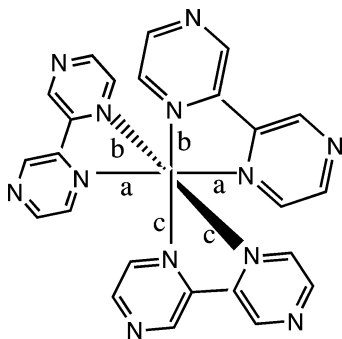
Figure 5. Bond names in the ^{3}MLCT(C_2) structure.

Table 4. Optimized B3LYP Geometries of [Ru(bpy)$_3$]$^{2+}$ and [Ru(bpz)$_3$]$^{2+}$ for ^{3}MC(C_2) Excited States and Atomic Spin Density[a]

	LL = bpy			LL = bpz		
bond length/angle	c	a	b	c	a	b
Ru−N	2.10	2.46	2.16	2.16	2.45	2.21
>C−N	1.36	1.35	1.36	1.34	1.35	1.35
>C−C<	1.47	1.48	1.48	1.48	1.48	1.48
C−N−C	118.8	119.4	119.4	118.3	118.3	117.6
N−Ru−N	77.5	71.8	71.8	77.5	71.5	71.0
N−Ru−N−N	83.3	83.0	83.6	82.0	89.6	89.6
N−>C−C<−N	−2.30	11.4	11.4	0.50	12.9	12.9
atomic spin density	0.06	0.05	0.05	0.14	0.03	0.03

[a] Bond distance (in angstroms) and angles (in degrees).

postulated to be [Ru^{II}(bpy)$_2$(η_1-bpy)]$^{2+}$, and it is a relatively long-lived species (80 μs).

From a theoretical point of view, Buchs and Daul[31] have calculated the energy of the lowest d−d transition within the Franck−Condon approximation for the [Ru(bpy)$_3$]$^{2+}$ complex. Assuming the same geometry as the ground state, they found that the ^{3}MC state should lie as much as 33000 cm^{-1} higher! TD-DFT results presented in the next section agree completely with this value. At the ground-state geometry, no ^{3}MC was found lying within the range 0−31000 cm^{-1} above the ground state.

Starting from a Hartree−Fock initial guess, an electron was put on the dπ_1* orbital, and a lengthening of two Ru−N bonds takes place during optimization in the BS1 basis set. As a result, two Ru−N bonds break to produce complexes with two monodentate ligands. This geometry was used with the larger basis set BS2, and an identical state was obtained. Inspection of the weak spin contamination by the mean of the $\langle S^2 \rangle$ expectation values (LL = bpy, 2.015; bpz, 2.010)

(31) Buchs, M.; Daul, C. L. *Chimia* **1998**, *52*, 163−166.

and inspection of the spin densities (last line of Table 4) show that the optimized state is of the metal-to-metal charge-transfer (^{3}MC) type. We observe a migration of a d electron from the Ru atom toward a dσ* orbital (Figure 2d). Population of this dσ* molecular orbital has profound consequences, as will be discussed below.

The resulting optimized geometry for [Ru^{II}(bpy)(η_1-bpy)$_2$]$^{2+}$ is shown schematically in Figure 7, and the principal geometrical parameters, which are reported in Table 4, show a structure with C_2 symmetry. Vibrational analysis indicates clearly that in each case the relaxed structures do not correspond exactly to true minima on the excited potential energy surface. For example, in the bpy case, three small imaginary frequencies (79.8i, 26.7i, and 22.4i cm^{-1}) were found. They correspond to rotations of the two monodentate bicycles around the remaining Ru−N bonds in opposite senses. These three vibrational modes do not lead to a dissociation of the molecule. The two optimized structures show a decoordination of two opposite sites, with two Ru−N bond lengths close to 2.4 Å, and the two monodentate LL ligands are rotated by about 12°. However, some differences
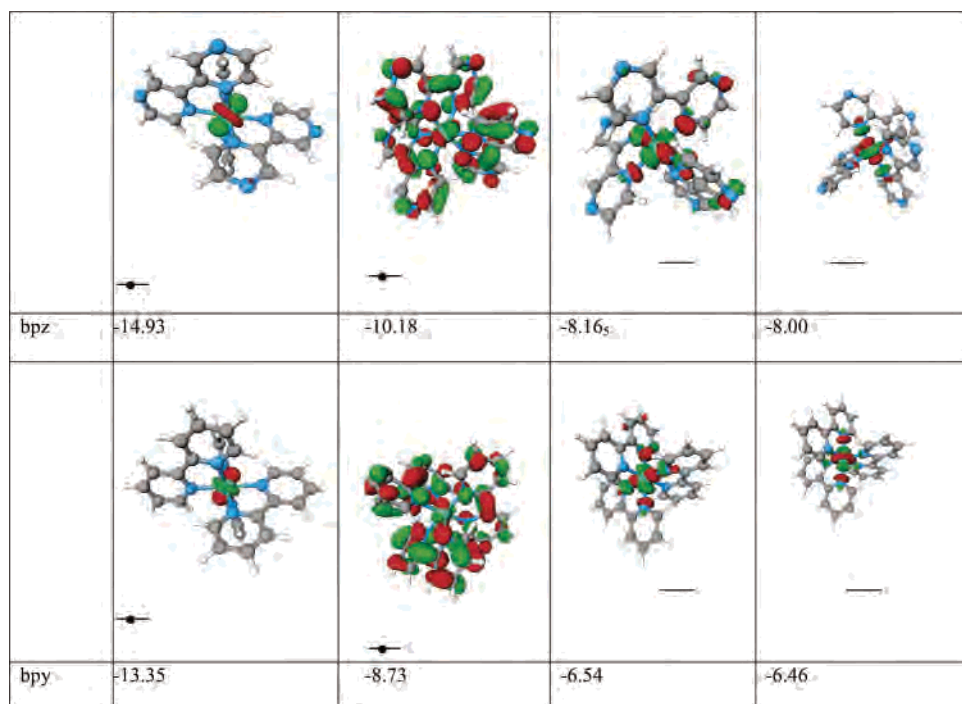
Figure 6. Schematic drawings of the d-block orbitals and the corresponding eigenvalues (eV) of the ^{3}MLCT state of C_2 symmetry for [Ru(bpy)$_3$]$^{2+}$ and [Ru(bpz)$_3$]$^{2+}$.

Figure 7. Bond labeling in the [Ru(bpz)$_3$]$^{2+}$ ^{3}MC structure (left). Drawing of the optimized [Ru(bpy)$_3$]$^{2+}$ ^{3}MC state structure (right).

between the two complexes can be noted. For the bpz system, the bond lengths between the metal and the N atom are larger, which implies that the ligands are less bounded to the metal. The dihedral angle N−Ru−N−N is also larger than that in the bpy complex, thereby offering a more facile approach for a solvent molecule.

These ^{3}MC states are quite close in energy to the ^{3}MLCT-(C_2) state, despite the qualitative change in the orbital excitations and the large geometrical differences. [Ru^{II}(bpy)-(η_1-bpy)$_2$]$^{2+}$ appeared slightly more stable than its ^{3}MLCT-(C_2) state by about 612 cm^{-1} (77 meV), whereas the [Ru^{II}(bpz)(η_1-bpz)$_2$]$^{2+}$ state is found to be slightly higher in energy by about 203 cm^{-1} (52 meV). For both complexes, the calculated energies of the three lowest triplet states are so close to each other that it is not possible to decide which of them is the lowest. Figure 8 gives a 3-D representation of the relevant frontier molecular orbitals. In the case of the [Ru(bpy)$_3$]$^{2+}$ complex, the two molecular orbitals for the unpaired electrons in the ^{3}MC state involve a Ru d$_{z^2}$ orbital and a dσ_2* orbital. In the case of the bipyrazine complex [Ru(bpz)$_3$]$^{2+}$, this excitation shows the migration of an

electron from a mixed d$_{xz}$/d$_{yz}$ orbital to the dσ_2* orbital. This different behavior surprised us, but even after several attempts, we could not obtain the same ^{3}MC state as that for the bipyridine complex. The π-antibonding character between the π orbital of the ligand and the d contribution of the atomic orbital leads to a fairly small metal−N bond lengthening. As a consequence of the increase of the Ru−N bond lengths during the geometry optimization, we observe a drastic diminution of the dσ* energy in such a way that this antibonding orbital becomes finally the HOMO, as shown in Figure 9. This behavior is consistent with the discussion presented by Pollack et al.[32] on the σ-antibonding character of such dσ* orbitals.

Rupture of the two bonds yields an intermediate with two coordination vacancies that are able to react with solvent molecules or to support photoisomerization. Indeed, during geometry optimization of the corresponding closed-shell [Ru^{II}(LL)(η_1-LL)$_2$]$^{2+}$, we reform the ground state, for both complexes.

6.2.2. TD-DFT. 6.2.2.1. TD-DFT/Ground State (GS). Absorption Properties. In Table 5, we report computed vertical excitation energies for the ground state for the two complexes and the composition of the corresponding excitation obtained, whose oscillator strength (f) is larger than 0.01. All of them are MLCT states of symmetry E, because they favor large transition moments. The calculated absorption spectra of [Ru(bpy)$_3$]$^{2+}$ and [Ru(bpz)$_3$]$^{2+}$ display common features. The agreement between the theoretical and experimental values is good. In both cases, the charge is transferred from the metallic center to bpy or bpz fragments. The

(32) (a) Pollack, C.; Rosa, A.; Baerends, E. J. *J. Am. Chem. Soc.* **1997**, *119*, 7324−7329. (b) Wilms, M. P.; Baerends, E. J.; Rosa, A.; Stufkens, D. J. *Inorg. Chem.* **1997**, *36*, 1541−1551.
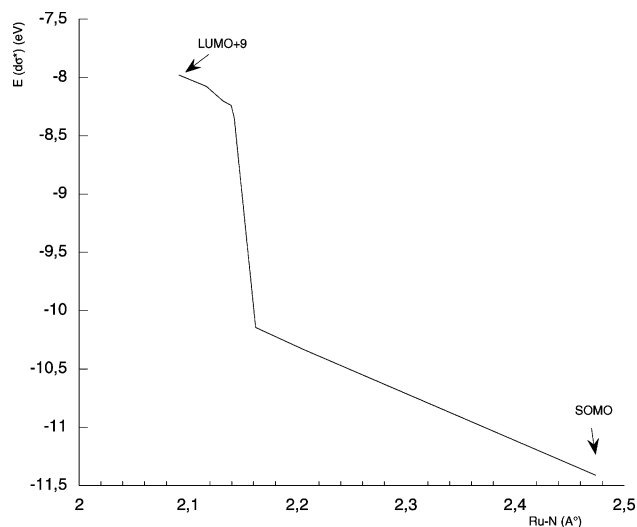
Figure 8. SOMO pairs.

Figure 9. Energy of the $d\sigma^*$ molecular orbital as a function of the metal–ligand bond length.

predicted transitions, with the largest oscillator strength at 2.88 and 2.77 eV (to be compared with experimental values of 2.74 and 2.81 eV), may be identified with the broad band of the absorption spectra, which has been assigned to a ^{1}-MLCT state. Juris et al.[33] have suggested that for the [Ru-(bpy)$_3$]$^{2+}$ complex the shoulders at 3.67 and 3.85 eV could be due to d → dσ^* (^{1}MC state) transitions. Our calculations do not show any ^{1}MC state in that region. These results are similar to those obtained by Broo and Lincoln[34] using INDO/SCI calculations on [Ru(bpy)$_3$]$^{2+}$.

(33) Juris, A.; Balzani, V.; Barigelletti, F.; Campana, S.; Belser, P.; von Zelewsky, A. *Coord. Chem. Rev.* **1988**, *84*, 85−277.
(34) Broo, A.; Lincoln, P. *Inorg. Chem.* **1997**, *36*, 2544−2553.

Probable Emissions. Whereas the comparison between vertically excited singlet states and the UV−visible spectrum is formally permitted, no direct correlation between the triplet excited states computed by the TD-DFT method and the UV−visible spectrum exists, with emission being the transition from a geometry-relaxed triplet state to an unrelaxed ground state. Nevertheless, among this set of triplet states, we can postulate that some of them can describe some probable transitions. Such comparisons seem reasonable if the geometrical reorganization between the excited triplet state and the ground state is small. Results presented in Table 6 show that in both complexes all of the transitions are dominated by ^{3}MLCT excitation, which corresponds to a single excitation from the set of d orbitals of the Ru atom, called d and dπ (see Figure 3 for the shape of orbitals), to dπ^* and π^* of the ligands. The two degenerate lowest bands correspond to a HOMO/LUMO+1 excitation (^{3}E states). On the other hand, no triplet excitations of metal-to-metal charge transfer (^{3}MC) are found by TD-DFT. In a Frank−Condon scheme, such excitations are surely too high at the geometry of the ground state.

At this stage, we can present all of our results concerning absorption and emission for both complexes in Table 7. It can be seen that, compared to experiments, our results are satisfactory.

6.2.2.2. TD-DFT/MLCT(D_3). Following the studies of Van Houten and Watts[26] and those of Rillema and co-workers,[7] the generally accepted scheme describing the nonradiative decay from the ^{3}MLCT level is the following: for most of these complexes, the ^{3}MC state is sufficiently low in energy to be responsible for the overall relaxation

Table 5. Computed TD-DFT Vertical Excitation Energies in Electronvolts and Oscillator Strengths (f) for Singlet States with $f > 0.01$ of [Ru(bpy)$_3$]$^{2+}$ and [Ru(bpz)$_3$]$^{2+}$ in Terms of Single Molecular Orbital Excitations with Percentages Larger than 10%

state labeling	LL = bpy (exptl value = 2.74 eV)			LL = bpz (exptl value = 2.81 eV)		
	transition energies (eV)	principal configuration	f	transition energies (eV)	principal configuration	f
^{1}E	2.70	$d\pi_2 \rightarrow \pi^*$ (−0.90) $d\pi_1 \rightarrow d\pi_2^*$ (0.29) $d\pi_2 \rightarrow d\pi_1^*$ (0.29)	0.0149	2.52	$d\pi_2 \rightarrow \pi^*$ (−0.90)	0.01534
^{1}E	2.70	$d\pi_1 \rightarrow \pi^*$ (−0.90) $d\pi_1 \rightarrow d\pi_1^*$ (0.29) $d\pi_2 \rightarrow d\pi_2^*$ (0.29)	0.0149	2.52	$d\pi_1 \rightarrow \pi^*$ (−0.90)	0.01534
^{1}E	2.89	$d\pi_1 \rightarrow \pi^*$ (0.4) $d\pi_1 \rightarrow d\pi_1^*$ (0.62) $d\pi_2 \rightarrow d\pi_2^*$ (0.62)	0.10713	2.77	$d\pi_2 \rightarrow \pi^*$ (−0.40) $d\pi_1 \rightarrow d\pi_1^*$ (0.62) $d\pi_2 \rightarrow d\pi_2^*$ (0.62)	0.10641
^{1}E	2.89	$d\pi_2 \rightarrow \pi_i^*$ (−0.4) $d\pi_1 \rightarrow d\pi_2^*$ (0.62) $d\pi_2 \rightarrow d\pi_1^*$ (0.62)	0.10713	2.77	$d\pi_1 \rightarrow \pi^*$ (0.4) $d\pi_1 \rightarrow d\pi_1^*$ (0.62) $d\pi_2 \rightarrow d\pi_1^*$ (0.62)	0.10641
^{1}E	3.67	$d \rightarrow \pi_i^*$ (0.96)	0.011			
^{1}E	3.84	$d\pi_1 \rightarrow \pi_i^*$ (−0.31) $d\pi_1 \rightarrow \pi_i^*$ (0.77) $d\pi_2 \rightarrow \pi_i^*$ (0.29) $d \rightarrow \pi_i^*$ (0.28)	0.018			
^{1}E	3.84	$d\pi_1 \rightarrow \pi_i^*$ (−0.28) $d\pi_2 \rightarrow \pi_i^*$ (−0.77) $d\pi_2 \rightarrow \pi_i^*$ (0.29) $d \rightarrow \pi_i^*$ (0.31)	0.018			

Table 6. Computed TD-DFT Vertical Excitation Energies in Electronvolts for the Six Lowest Triplet States of [Ru(bpy)$_3$]$^{2+}$ and [Ru(bpz)$_3$]$^{2+}$ in Terms of Single Molecular Orbital Excitations with Percentages Larger than 20%

LL = bpy			LL = bpz		
transition energies	state labeling	principal configuration	transition energies	state labeling	principal configuration
2.28(5)	^{3}E	$d \rightarrow d\pi_1^*$ (−0.91)	2.13	^{3}E	$d \rightarrow d\pi_1^*$ (0.8) $d\pi_1 \rightarrow \pi^*$ (0.32) $d\pi_1 \rightarrow d\pi_2^*$ (−0.23) $d\pi_2 \rightarrow d\pi_2^*$ (−0.24)
2.28(5)	^{3}E	$d \rightarrow d\pi_2^*$ (0.91)	2.13	^{3}E	$d\pi_1 \rightarrow \pi^*$ (0.8) $d\pi_2 \rightarrow \pi^*$ (0.32) $d\pi_2 \rightarrow d\pi_2^*$ (0.24) $d \rightarrow d\pi_2^*$ (0.8)
2.31	^{3}A$_2$	$d \rightarrow \pi^*$ (−0.92)	2.13	^{3}A$_1$	$d\pi_1 \rightarrow d\pi_2^*$ (0.68) $d\pi_2 \rightarrow d\pi_2^*$ (0.68)
2.35	^{3}A$_1$	$d\pi_1 \rightarrow d\pi_2^*$ (0.67) $d\pi_2 \rightarrow d\pi_2^*$ (0.67)	2.13	^{3}A$_2$	$d \rightarrow \pi^*$ (0.83) $d\pi_2 \rightarrow d\pi_2^*$ (0.29) $d\pi_1 \rightarrow d\pi_1^*$ (0.29)
2.46	^{3}E	$d\pi_2 \rightarrow \pi^*$ (−0.49) $d\pi_2 \rightarrow d\pi_1^*$ (0.57) $d\pi_1 \rightarrow d\pi_2^*$ (0.57)	2.25	^{3}E	$d\pi_2 \rightarrow \pi^*$ (0.6) $d\pi_2 \rightarrow d\pi_2^*$ (0.54) $d\pi_1 \rightarrow d\pi_1^*$ (−0.54)
2.46	^{3}E	$d\pi_1 \rightarrow \pi^*$ (−0.49) $d\pi_1 \rightarrow d\pi_2^*$ (−0.57) $d\pi_2 \rightarrow d\pi_2^*$ (0.57)	2.25	^{3}E	$d\pi_1 \rightarrow \pi^*$ (0.6) $d\pi_1 \rightarrow d\pi_2^*$ (0.54) $d\pi_2 \rightarrow d\pi_1^*$ (−0.54)

process. However, in a few cases, the energy gap between the ^{3}MLCT levels and the ^{3}MC, i.e., ΔE(^{3}MC), is too large, and an alternative scheme is necessary to describe the nonradiative decay. This alternative scheme involved another low-lying MLCT state named the "fourth ^{3}MLCT". Sykora and Kincaid[35] have proven with an experimental study on a series of heteroleptic complexes that both the ^{3}MC state and the fourth MLCT states can contribute to the nonradiative decay. They revealed that the relative contributions depend on the donor strength of the spectator ligand. The results of TD-DFT calculations from the low-lying ^{3}MLCT(D_3) are presented in Figure 10. For both complexes, the transitions obtained with our calculations with TD-DFT calculations at

the optimal geometry of the ^{3}MLCT(D_3) state correspond to $d \rightarrow d\sigma^*$ and to $d \rightarrow d$ excitations that coincide with the experimental data. For the two complexes, the set of degenerate low-lying states coincides with the three ^{3}MLCT states predicted by Van Houtten and Watts.[26] Our calculations predict that these low-lying excited states lie within 0.32 eV ($\approx$2600 cm^{-1}) in both cases. These values agree well with the experimental value[26] of 3000 cm^{-1}.

We note one significant difference between the excited-state manifold of the two complexes. For the bipyridine case, a ^{3}MLCT state appears after the three first ^{3}MLCT levels. This state is well separated from the others. We associate this state with the fourth ^{3}MLCT state discussed above. The calculated energy gap between the first ^{3}MLCT cluster and

(35) Sykora, M.; Kincaid, J. R. *Inorg. Chem.* **1995**, *34*, 5852−5856.

Table 7. TD-DFT Values Computed Using Ground-State Geometries and Δ-SCF Energies Computed Using Optimized ^{3}MLCT(D_3) Geometries

		TD-DFT		Δ-SCF/GS^a		Δ-SCF/FC^b	exptl[24,25]
		this work	Xie et al.*		this work		
$[Ru(bpy)_3]^{2+}$	absorption	2.88 (430)	2.99 (415)				2.74 (452)
	emission	2.28 (543)^c	2.26 (548)	2.23	^{3}MLCT(D_3)	2.13 (582)	2.13 (582)
				2.22	^{3}MLCT(C_2)	2.10 (590)	
				2.14	^{3}MC	1.08	
$[Ru(bpz)_3]^{2+}$	absorption	2.77 (447)					2.81 (441)
	emission^c	2.13 (582)		2.30	^{3}MLCT(D_3)	2.21 (561)	2.16 (573)
				2.29	^{3}MLCT(C_2)	2.18 (568)	
				2.34	^{3}MC	0.96	

^{a} Δ-SCF/GS is obtained from the difference between the energy of the optimal geometry of the excited state and the energy of the ground state. ^{b} Δ-SCF/FC is obtained from the difference between the energy of the optimal geometry of the triplet excited state and the single-point energy of the singlet closed-shell state at the geometry of the corresponding excited states. ^{c} See precaution with the term emission for TD-DFT results in the full text.
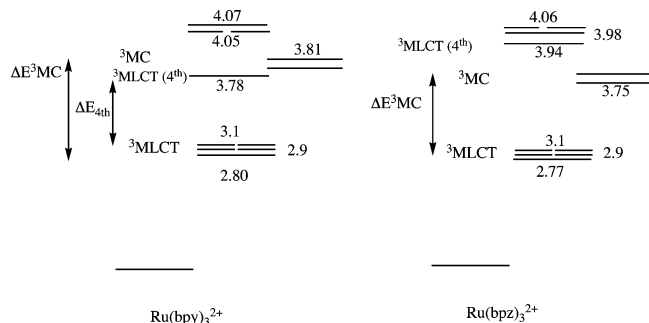

Figure 10. Schematic representation of the manifold of the excited states of the $[Ru(bpz)_3]^{2+}$ and $[Ru(bpy)_3]^{2+}$ complexes obtained at ^{3}MLCT(D_3) geometry.

the fourth ^{3}MLCT (ΔE_{fourth}) is 0.663 eV (5348 cm^{-1}) in the case of the bpy ligand. However, for the $[Ru(bpz)_3]^{2+}$ complex, the so-called fourth MLCT state does not appear at the same place. It should be pointed out that our results reproduce nicely the experimental predictions that stipulate that in the case of the $[Ru(bpz)_3]^{2+}$ complex $\Delta E(^3MC)$ is so small ($\approx$0.48 eV or $\approx$3900 cm^{-1}) that no evidence of the existence of a fourth state was found. While the ^{3}MC states corresponding to d → dσ* excitations are probably rejected in the upper part of the spectrum when TD-DFT calculations are carried out at the geometry of the ground state, at their excited geometry, calculated excitations give rise to two degenerate ^{3}MC states. For both complexes, these states appear at *ca.* 0.7 eV ($\approx$5600 cm^{-1}) above the lowest ^{3}MLCT set state. These values must be compared to the 3600 cm^{-1} predicted by the models used to interpret experimental data.[35] For both complexes, all of the excited states obtained with higher energy are of the ^{3}MLCT type. In the case of the $[Ru(bpz)_3]^{2+}$ complex, the so-called fourth state is destabilized and lies at 0.2 eV ($\approx$1600 cm^{-1}) above the two ^{3}MC states.

TD-DFT excited-state results are consistent with the experimental trends obtained by Sykora and Kincaid.[35] Involvement of the fourth state is necessary to understand the experimental decay rate of $[Ru(bpy)_3]^{2+}$, yet the TD-DFT method clearly distinguishes a ^{3}MLCT state that we have identified as the so-called fourth state. In the same way, the absence of the fourth state between the ^{3}MLCT cluster and ^{3}MC states in our calculation agrees with the unique deactivation pathway of the ^{3}MLCT state by the ^{3}MC route, without observation of the fourth state in $[Ru(bpz)_3]^{2+}$.

7. Conclusion and Perspectives

The aim of this work was to see if differences in the relative energies of the various excited states of $[Ru(bpy)_3]^{2+}$ and $[Ru(bpz)_3]^{2+}$ could explain their differences in reactivity toward metalloproteins. The absorption spectra can be reproduced very well by the TD-DFT method. Both molecules are excited toward a ^{1}MLCT state that has C_2 symmetry at its optimum geometry. From these states, the molecules are de-excited, via nonradiative transfers, toward one or several triplet states whose nature had not been convincingly explained before this work. We have been able to characterize several different electronic states with different spatial symmetries, and optimize their geometry, using the DFT method. Two ^{3}MLCT states have been found for both molecules. The first one, with D_3 symmetry, thus having one electron spread over three ligands, is a true minimum and is found at the right energetic level compared with the experimental spectra. The second has C_2 symmetry, and as a consequence one ligand is more highly charged than the two others: it is also a true minimum, and it lies just a few reciprocal centimeters below the D_3 state. The quasi-degeneracy of these two states readily explains the experimental observation that, under some circumstances, these states are described as D_3, whereas under other conditions, they are described as C_2. For the C_2 states, the three components and the norm of the dipole moment do not really imply that an electron is totally localized on a single ligand, as is often presented for these states. However, a third state is also found lying at the same energy; this is the main result of this work. This state, of MC nature (d−d), also has C_2 symmetry, but it has a very different geometry. Placing an electron in the dσ* orbital, which is strongly antibonding, leads to the decoordination of two opposite (trans) N atoms from the metal. Two bipyridine or bipyrazine ligands are now singly coordinated to the metal, which is only four-coordinated: this structure thus leaves room for solvent molecules to approach the metal and to form reactive intermediates. Because of the very antibonding nature of the dσ* orbital, this state lies very high in energy at the geometry of the ground state, and it cannot be found in the TD-DFT spectrum of the 20 lowest states. However, by performing a TD-DFT study on the ^{3}MLCT state, at its own geometry, we were able to find this four-coordinated state in between several ^{3}MLCT states, all of them lying within 3000 cm^{-1}.

Within such a narrow energetic interval, it is probable that many interconversion processes occur. It also seems more probable that this is the MC state that reacts with other molecules. At this stage, no dramatic differences between bpy and bpz emerge from our results. It should be noted, however, that the MC state is slightly lower in the manifold of triplet states for bpz, and thus more interconversion from the MLCT states toward the MC state could occur for this ligand.

A complete vibrational analysis will be presented for all states of both molecules in a forthcoming publication. Much work remains to be done concerning the MC state. For instance, the reactivity of these ^{3}MC states with solvent molecules, i.e., explicit water molecules, is being studied. Such reactivity should be associated with some very interesting intermediates, as mentioned in the work of Thomson et al.[30] For example, it is not yet clear why the existence of complexes with only one exogenous ligand has been widely discussed if there really are *two* decoordinated sites. In their ground states, these polypyridyl complexes are chiral molecules. The MC states may be involved as crucial intermediates in the photoracemization process.